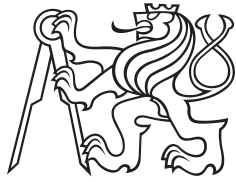


Research task



Czech
Technical
University
in Prague

F4

Faculty of Nuclear Sciences and Physical Engineering
Department of physics

Influence of energy of neutrons, source geometry and background hard-X-rays on the neutron flux measurements at tokamaks

Bc. Lukáš Lobko

Supervisor: Ing. Ondřej Ficker
June 2020



Katedra: fyziky

Akademický rok:

2019/2020

VÝZKUMNÝ ÚKOL

Student: Bc. Lukáš Lobko

Studijní program: Aplikace přírodních věd

Obor: Fyzika a technika termojaderné fúze

Vedoucí úkolu: Ing. Ondřej Ficker
Ústav fyziky plazmatu AV ČR, Za Slovankou 1782/3, 182 00 Praha 8
FJFI ČVUT v Praze, Břehová 78/7, 115 19 Praha 1

Název úkolu (česky/anglicky):

Vliv energií neutronů, geometrie zdroje a pozadí tvrdého rentgenového záření na měření neutronových toků na tokamacích.

Influence of energy of neutrons, source geometry and background hard-X-rays on the neutron flux measurements at tokamaks.

Pokyny pro vypracování:

- Pokračování vývoje software pro diskriminaci píků u scintilačních detektorů.
- Analytické ověření vlivu toroidální geometrie zdroje neutronů na množství detekovaných neutronů.
- Výpočet vlivu distribuční funkce neutronů v energiích na množství detekovaných neutronů vzhledem k vlastnostem detektoru.
- Základní rešerše kódů pro výpočet transportu neutronů (MCNP6, atd.).
- Účast na měřeních neutronů na tokamaku COMPASS.
- Hledání závislostí mezi počtem neutronů a parametry plazmatu.

Výzkumný úkol bude vypracován v anglickém jazyce.

Součástí zadání výzkumného úkolu je jeho uložení na webové stránky katedry fyziky.

- Literatura:**
- [1] L. Bertalot, et al.: Fusion neutron diagnostics on ITER tokamak, JINST 7 C04012, 2012
 - [2] M. F. L'Annunziata: Handbook of Radioactivity Analysis, 3rd Ed., Elsevier, 2012
 - [3] C. J. Werner (editor): MCNP Users Manual - Code Version 6.2, [LA-UR-17-29981](#), 2017
 - [4] Lintereur, Azaree T. et al.: Neutron and Gamma Ray Pulse Shape Discrimination with Polyvinyltoluene, 2012

Datum zadání: 25.10.2019

.....

Datum odevzdání: 26.06.2020

vedoucí katedry

Acknowledgements

Many thanks to my supervisor Ing. Ondřej Ficker for guiding my research task, for his important advices and comments.

Declaration

I declare that I have prepared the submitted work independently and that I have listed all the used literature.

In Prague, 20. June 2020

Abstract

This work follows the Bachelor thesis of the author and thus develops horizons regarding practical use of neutron diagnostics on the COMPASS tokamak. Specially this report is focused on the detection of individual neutron and HXR peaks measured by NuDET scintillation detector. This work presents measurements and data analysis from two campaigns (CC21.06; CC22.01) on the COMPASS tokamak. Data analysis leads to several results: calculation of neutron attenuation coefficient of the main shielding wall, estimation of the absorbed dose of radiation for COMPASS and COMPASS-U, photoneutrons detection, the proof of the presence of high energy runaway electrons and finally the estimation of total amount of HXR photons with energies higher than 2,2 MeV generated by runaway electrons.

Keywords: neutron peaks, HXR peaks, neutron/ γ discrimination, wall shielding, absorbed dose of radiation, runaway electrons, photoneutrons, COMPASS, COMPASS-U

Supervisor: Ing. Ondřej Ficker
IPP of the Czech Academy of Sciences,
Za Slovankou 1782/3,
Prague 8

Abstrakt

Tato práce navazuje na bakalářskou práci autora a rozvíjí tak obzory ohledně praktického použití neutronové diagnostiky na tokamaku COMPASS. Speciálně se zaměřuje na detekci jednotlivých neutronových a HXR píků měřených scintilačním detektorem NuDET. Práce prezentuje měření a zpracování dat ze dvou kampaní (CC21.06; CC22.01) na tokamaku COMPASS. Analýza dat vede k několika výsledkům: určení neutronového útlumového koeficientu hlavní stínící zdi, odhad absorbované dávky záření pro COMPASS a COMPASS-U, detekce fotoneutronů, důkaz o přítomnosti vysokoenergetických ubíhajících elektronů a nakonec odhad celkového množství HXR fotonů o energiích vyšších než 2,2 MeV generovaných ubíhajícími elektrony.

Klíčová slova: neutronové píky, HXR píky, neutron/ γ diskriminace, stínění, absorbovaná dávka záření, ubíhající elektrony, fotoneutrony, COMPASS, COMPASS-U

Překlad názvu: Vliv energií neutronů, geometrie zdroje a pozadí tvrdého rentgenového záření na měření neutronových toků na tokamacích

Contents

Introduction	1	2.3.1 Equivalent dose of the COMPASS tokamak	12
1 Theoretical background	3	2.3.2 Equivalent dose of the COMPASS-U tokamak	12
1.1 Cross section of the nuclear reaction	3	3 Measurement of neutrons on the HXR background	15
1.2 Scintillation detector NuDET . . .	4	3.1 Experimental setup	15
1.3 Absorbed dose and equivalent dose	5	3.2 Measurement of HXR counts . . .	16
1.4 Fourier transform	5	3.2.1 Equivalent dose from RE discharges	16
1.5 Runaway electrons	6	3.3 Neutrons discovery	18
1.6 Deuterium gas puff	6	3.4 Source of neutrons	19
2 Measurement of neutron fluxes behind the main wall around the COMPASS tokamak	7	3.4.1 Neutron/HXR discrimination	19
2.1 Experimental setup	7	3.4.2 Neutron counts	20
2.2 Estimation of neutron wall attenuation coefficient	8	3.4.3 Deuterium gas puff	23
2.2.1 Measurement technique	8	Conclusion	25
2.2.2 Results	10	Appendix	27
2.3 Equivalent dose of neutron radiation	10	Analytical verification of influence of toroidal neutron source geometry on the detected neutron fluxes	27

Influence of energy distribution function of neutrons and detector attributes on the detected neutron fluxes	28
Neutron transport in the COMPASS-U tokamak	29
Bibliography	31

Figures

1.1 Cross section of neutron-lithium nuclear reaction, [1].	4	3.6 Spectral decomposition of neutron ultraslow component.	21
2.1 Example of the piled-up neutron signal from the EJ-410, discharge #19868.	9	3.7 Application of 100 kHz lowpass bandwidth filter on HXR peak. . . .	21
2.2 Schematic picture illustrates two different situations - inside/outside measurement.	9	3.8 Application of 100 kHz lowpass bandwidth filter on neutron peak. .	22
2.3 Linear fit for inside measurement.	11	3.9 Cross section of the $D(\gamma, n)^1H$ reaction, [3].	23
2.4 Linear fit for outside measurement.	11	3.10 Radial neutron profile of a toroidal sources in a size of the COMPASS tokamak plasma, author: Ondřej Ficker.	28
2.5 Reduction of absorbed dose by ordinary concrete shielding from 3 MeV incident neutrons, [2].	14	3.11 Dependency of the neutron count rate on the mean energy of neutrons for the three different reactions ($^6Li(n, \alpha)T$; $^3He(n, p)^3H$; $n - ^4He$ recoil), author: Ondřej Ficker. . . .	29
3.1 Example of the cluster of HXR peaks.	17	3.12 Order of magnitude of neutron fluxes per cm^2 per year of the COMPASS-U tokamak, author: group of researchers from the Institute of Nuclear Research of the Polish Academy of Sciences.	30
3.2 Example of HXR peaks (enlarged area).	17		
3.3 Example of the HXR peak.	18		
3.4 Example of the neutron peak. . . .	19		
3.5 Spectral decomposition of HXR peak.	20		

Tables

3.1 Time decays of HXR and neutron peak.....	19
3.2 The list of discharges with high neutron fluxes.	22
3.3 The list of discharges without or with very low neutron fluxes.	22



Introduction

Research in the area of thermonuclear fusion is gaining in importance with each passing year. With the completion of the forthcoming thermonuclear reactor ITER in France, thermonuclear fusion is enjoying increasing interest in media. In a few decades the energy from thermonuclear reactors should help significantly with the problems connected with the global warming phenomenon and closing coal and even fission nuclear power plants, although there is yet no way, how to replace them effectively given the evergrowing world energy consumption.

With increasing size and with higher power of the auxiliary plasma heating of the new tokamaks like ITER, COMPASS-U, the fusion power mediated by fusion neutrons rapidly increases. Thus neutron diagnostics is gaining in importance. On the ITER tokamak, extensive neutron diagnostics will be installed for the monitoring of the fusion power.

Existing neutron diagnostics on the tokamaks consists of a few types of detectors like proportional counters, fission chambers, activation foils. Especially scintillation detectors are very often an important part of neutron diagnostics on the tokamaks. Neutron detectors on small devices are often operated outside the single event counting regime and give only relative information on the fluxes.

In this paper, we focus on measurement with NuDET scintillation detector on the COMPASS tokamak. This work shows the possibilities of NuDET detector to measure individual neutron and γ peaks. With measurement of these individual signals we were able to calculate a few interesting values, which would probably not be otherwise possible to gain or only by very complicated way.

The first chapter contains basic theoretical background in the selected areas used in the practical part. Then, NuDET measurements and data analysis itself from two different campaigns conducted recently on the COMPASS

tokamak are presented. The first measurement is focused on detection of individual neutron peaks during standard NBI discharges and leads to the estimation of neutron attenuation coefficient of the main shielding wall and the estimation of absorbed dose for COMPASS and COMPASS-U is made, too. Second measurement is focused on individual HXR/ γ peaks detection during RE campaign. Detailed data analysis leads to unexpected detection of photoneutrons with interesting results.

Chapter 1

Theoretical background

This chapter contains basic informations about the mathematical concepts and physical phenomena used in the chapters 2 and 3 and thus can help the reader in understanding the text.

1.1 Cross section of the nuclear reaction

The knowledge of nuclear reactions respectively the conditions, under which nuclear reactions occur or occur often enough, is the key information. For example, the thermonuclear fusion research is trying somehow to reach these optimal conditions of especially D-D and D-T nuclear reactions. The main parameter, which describes these conditions, is the cross section σ of nuclear reaction defined

$$\sigma = \frac{R}{N\Gamma}, \quad (1.1)$$

where R [s^{-1}] is a frequency of nuclear reaction, N [–] is the number of the atomic nuclei of the motionless target and Γ [$\text{m}^{-2}\text{s}^{-1}$] is the flux of shelling particles hitting the target. The unit of σ is m^2 , it is imaginable approximately like the effective area, which the particle must strike in order to occur the nuclear reaction. Because of very small values the usually used unit is barn ($1 \text{ barn} = 1 \cdot 10^{-28} \text{ m}^2$), see e.g. [4].

1.2 Scintillation detector NuDET

Scintillation detector NuDET, [5], from the company Nuvia is the main tool, with which we have measured all the data in this report. The core of the detector is composed of the small scintillation crystal ZnS(Ag) in the shape of a thin cylinder with thickness 4 mm and diameter 40 mm. Scintillation crystal is connected to a PMT. On the detection area of the crystal a thin layer of ^6LiF is applied. This layer converts neutrons to the charged particles through the nuclear reaction



The cross section σ of this reaction varies in a wide range, from 1000 barn to less than 1 barn, fig. 1.1.

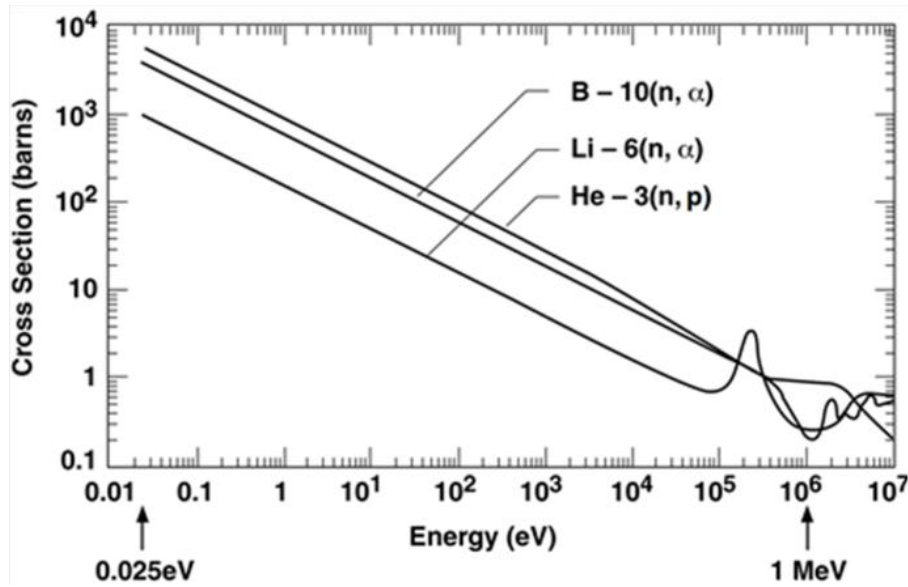


Figure 1.1: Cross section of neutron-lithium nuclear reaction, [1].

With the appropriate oscilloscope or another A/D converting device this detector is able to measure individual neutron and HXR/ γ photons and even distinguish between them, as will be shown in the next chapters.

The NuDET sensitivity to the neutrons is 4.5 cps/nv for thermal neutrons ($E = 0,025$ eV), declared by manufacturer. If we consider detection area of this detector, it means, that the sensitivity for detecting thermal neutrons is 35,8 %. Every third neutron, which strikes the detector, is registered. From the definition of the cross section σ , eq. 1.1, we can simply calculate, that the number of lithium nuclei in the NuDET detector is $N = 4,5 \cdot 10^{21}$. Using this knowledge and the cross section of neutron-lithium reaction, fig. 1.1, we can recalculate the NuDET sensitivity to the neutrons with any energy.

1.3 Absorbed dose and equivalent dose

For the calculation of the radiation impact on the living tissue the quantity named absorbed dose D must be first determined. D indicates, how much energy was absorbed in 1 kilogram of the given material (body, tissue, organ, ...). The unit is Gray (Gy). It is obvious, that $1 \text{ Gy} = 1 \frac{\text{J}}{\text{kg}}$.

However, the true biological impact doesn't just matter only on the amount of absorbed energy, but it depends on the kind of the radiation, too. For this purpose another quantity named equivalent dose H was introduced like

$$H = W_R \cdot D, \quad (1.3)$$

where W_R is the „radiation weighting factor“. W_R is dimensionless quantity and the default value is $W_R = 1$ for the HXR/ γ radiation. The factor is larger for some other types of radiation. For example $W_R = 10$ for neutrons with energies between (10 keV - 100 keV). This means, that these neutrons are ten times more dangerous for living tissue than HXR/ γ radiation, when the same dose is absorbed. The unit of H is Sievert (Sv). Sievert is mathematically the same unit as Gray, but the difference in the meaning is obvious. For more details see [6].

1.4 Fourier transform

Generally we can imagine some function $z(t)$ like continuous superposition of the functions sine and cosine with different frequencies f :

$$z(t) = \frac{1}{2\pi} \int_{-\infty}^{+\infty} Z(\omega) e^{i\omega t} d\omega, \quad (1.4)$$

where $\omega = 2\pi f$. This is called the inverse Fourier transform. Usually we are interested, which frequencies are dominant for the given function $z(t)$. For this purpose, the function $Z(\omega)$ called Fourier transform needs to be calculated. Fourier transform can be expressed like

$$Z(\omega) = \int_{-\infty}^{+\infty} z(t) e^{-i\omega t} dt. \quad (1.5)$$

In other words, Fourier transform converts the function $z(t)$ from the time domain to the frequency domain (frequency spectrum).

Our function of interest is the exponential function $z(t) = A \cdot e^{-\frac{t}{\tau}}$. By using eq. 1.5 we can simply gain

$$Z(\omega) = \frac{A}{\frac{1}{\tau} + i\omega} = \frac{A(\frac{1}{\tau} - i\omega)}{\frac{1}{\tau^2} + \omega^2}. \quad (1.6)$$

The absolute value gives us the frequency spectrum of the exponential function $z(t)$

$$|Z(\omega)| = \frac{A}{\sqrt{\frac{1}{\tau^2} + (2\pi f)^2}}. \quad (1.7)$$

For more details about Fourier transform see [7].

1.5 Runaway electrons

One of the up to date hot topics in the fusion tokamak research are runaway electrons. Runaway electrons are electrons, which are accelerated to the relativistic velocities. REs usually appear during disruptions in the tokamaks, when strong electric field is suddenly induced. Basically electrons are more accelerated than braked by thermal collisions and so runaway electrons arise. Beam of the REs can damage plasma facing components. In chapter 3, we are focusing on the measurement of HXR radiation caused by the collisions of REs with plasma facing components. For detailed information about physics of runaway electrons in tokamaks (mechanisms of origin, ...) see e.g. [8, 9].

1.6 Deuterium gas puff

During disruption and generation of runaway electrons, different mechanisms, how to mitigate RE beam to cause as little damage as possible, are tested. One of these mechanisms is the additional gas injection during and after the disruption. Standardly argon, neon or krypton gas puff is used to mitigate the RE beam. On COMPASS as well as on other tokamaks, a new approach - consisting of primary Ar or Ne injection followed by a secondary deuterium gas injection has been recently tested. It generally seems, that this combination of noble gases and deuterium gas puff is better than the gas puff consisting of higher amount of noble gas due to better positional stability of RE beam and perhaps also smaller acceleration of RE due to smaller current decay rate. For detailed information about noble gas puff on the tokamak COMPASS see the paper [10].

Chapter 2

Measurement of neutron fluxes behind the main wall around the COMPASS tokamak

In the next year the Institute of Plasma Physics will start to build a new tokamak COMPASS Upgrade. This tokamak will be built in the same place instead of the COMPASS tokamak. It is expected, that COMPASS-U will have up to factor of $\sim 10^4$ higher neutron fluxes than COMPASS. It can thus be assumed, that existing wall shielding would not be sufficient. In this chapter the measurement of neutron fluxes behind the main shielding wall of the COMPASS experimental hall is presented. The results lead to determine of the neutron attenuation coefficient of the COMPASS shielding wall. Then the equivalent dose of neutron radiation in the neighbourhood of the COMPASS and COMPASS-U tokamak experimental hall is estimated.

2.1 Experimental setup

The measurement was performed in December 2019 during campaign CC21.06 between discharges #19850 - #19917. We have used the neutron scintillation detector NuDET placed behind the main wall around the tokamak COMPASS. For data collection we have used OWON oscilloscope XDS3202A.

To estimate neutron wall attenuation coefficient, data measured by the same detector NuDET connected to the different setup (oscilloscope NI PXI 5114) was also processed. The detector in this case was measuring neutron fluxes in May 2018 during campaign CC19.05 in the range of discharges

#16893 - #17099 inside the experimental hall of the COMPASS tokamak.

■ 2.2 Estimation of neutron wall attenuation coefficient

The main shielding wall around the COMPASS tokamak is made from concrete with a thickness of 60 cm.

■ 2.2.1 Measurement technique

It would be relatively easy to gain neutron wall attenuation coefficient, if we would have measured neutron counts inside and outside of the wall at the same time (in the same discharges). But due to technical issues this „double measurement“ was not realised. However, it appeared, that there is another way, how to work around this problem and use neutron counts inside and outside the hall from different discharges.

Besides NuDET detector, which is often used for special measurements like this, neutron diagnostic on the COMPASS uses another scintillation detector EJ-410 from the Eljen Technology company. This detector does not measure individual neutron counts (due to parameters of the data acquisition system ATCA 2). The signal consists of pile-uping of many individual neutron peaks, as we can see in the figure 2.1. But it's quite obvious, that the integral of the signal is proportional to the number of neutron counts. Another important fact is, that the detector EJ-410 operated with the same setup (always in the same position around tokamak, with the same lead shielding, data acquisition system, with fixed voltage on PMT, ...). Due to these two facts (signal proportional to number of counts, stable setup) it was clearly shown up, [11], that we can use integral of the EJ-410 signal as a figure of merit. Thus we can compare neutron counts from different discharges.

The principle is schematically shown in the figure 2.2. All we need is to determine (purple) linear curves of dependency of neutron counts on the integral of EJ-410 in the case of a detector inside the hall with tokamak and in the case when detector was operated outside, too. These linear curves

$$c_i = k_1 \cdot I, \quad (2.1)$$

$$c_o = k_2 \cdot I, \quad (2.2)$$

where c_i , c_o are number of neutron counts inside (outside) the hall, I is the integral of EJ-410 signal, determine parameters k_1 , k_2 . Their ratio equals to

neutron wall attenuation coefficient K_n

$$\frac{k_1}{k_2} = \frac{c_i}{c_o} \equiv K_n. \quad (2.3)$$

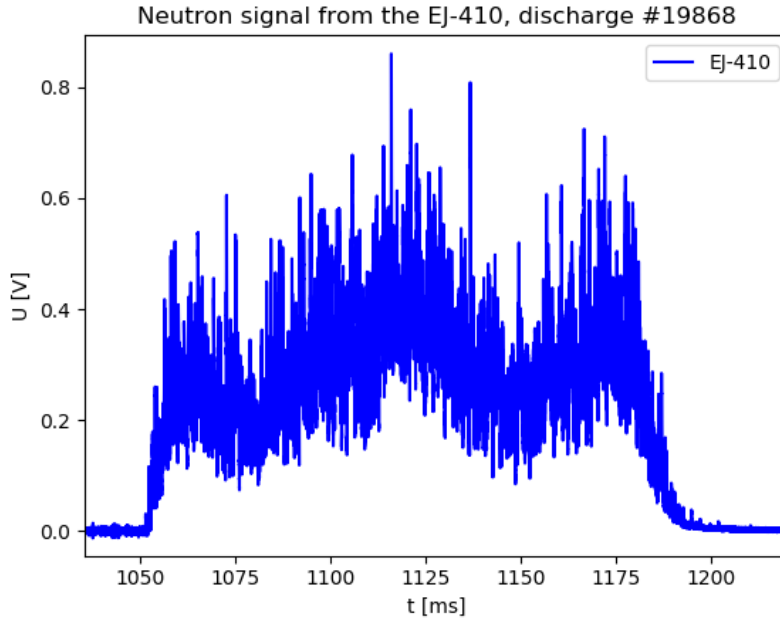


Figure 2.1: Example of the piled-up neutron signal from the EJ-410, discharge #19868.

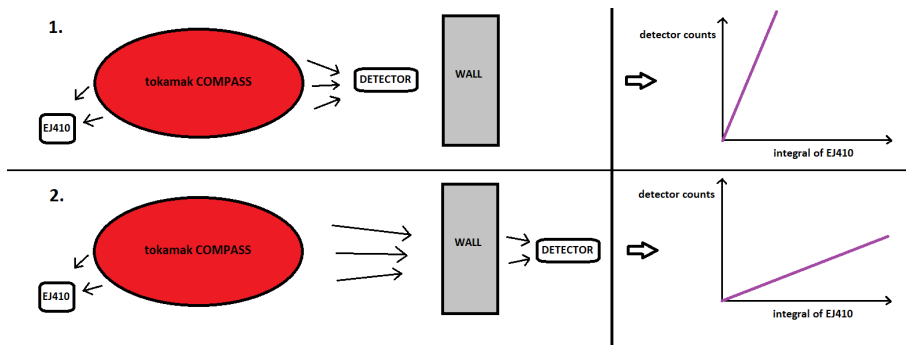


Figure 2.2: Schematic picture illustrates two different situations - inside/outside measurement.

■ 2.2.2 Results

Figure 2.3 shows individual discharges from campaign CC19.05 conducted in May 2018, when NuDET detector was placed inside the hall with COMPASS tokamak. We can see quite obvious linear dependence. Final linear fit (purple) was calculated as

$$c_i = (334, 22 \pm 7, 37) \cdot I. \quad (2.4)$$

Figure 2.4 shows individual discharges from campaign CC21.06 conducted in December 2019, when NuDET detector was placed outside the hall with COMPASS tokamak. There was less usable discharges for our purpose, but linear dependence is still visible. Final linear fit (purple) was calculated as

$$c_o = (4, 00 \pm 0, 13) \cdot I. \quad (2.5)$$

Finally neutron wall attenuation coefficient K_n defined in eq. 2.3 was calculated as

$$K_n = 83, 56 \pm 3, 28 \simeq 84. \quad (2.6)$$

This number means, that for every neutron, which passed through the wall, there were 84 neutrons absorbed in the shielding wall or reflected back to the interior of the experimental hall. The bigger the K_n is, the better the wall shields surrounding systems and workers. The main factor, which was not taken into account, is probably the influence of the wall on neutron energy spectra. The concrete shielding wall naturally moderates neutrons and thus neutron capture rate by lithium in NuDET detector can dramatically increase, as we can see in the figure 1.1. So this result should be better understood as the bottom estimation of neutron wall attenuation ability (in the meaning of minimal wall shielding ability).

■ 2.3 Equivalent dose of neutron radiation

Knowledge of the neutron energy spectra, to which the detector is exposed, is the key information for correct determination of neutron fluxes and thus for calculating equivalent dose. It is due to a wide range of the value of the cross section for the reaction of neutron with lithium. But we can calculate very strong upper estimate of the equivalent dose, which worker will be exposed to behind the wall of the tokamak.

The assumptions are as follows:

1. 1500 discharges during a year, all with 30000 neutron counts on NuDET inside. This is a bit higher than maximum measured neutron flux in May 2018 (maximum was cca 27 000 neutron counts).
2. Neutron wall attenuation coefficient $K_n = 84$. As stated above, the true

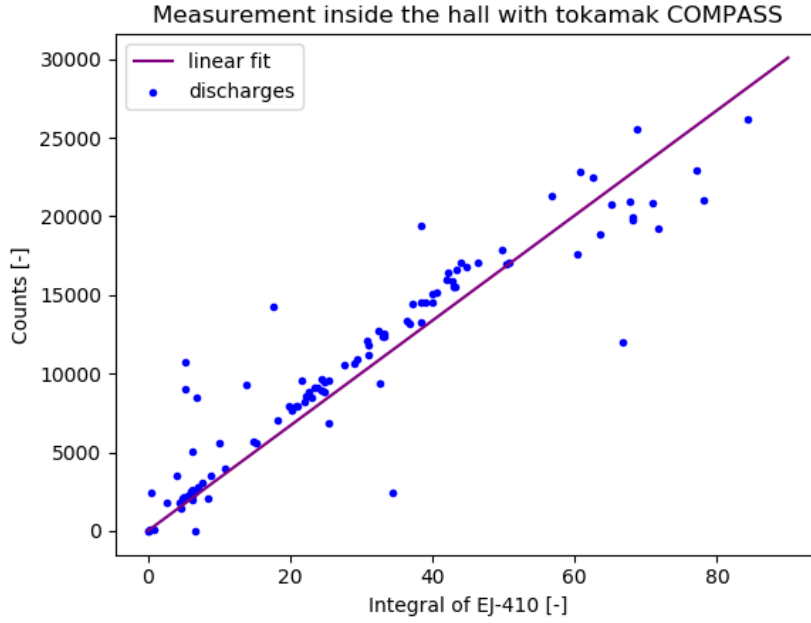


Figure 2.3: Linear fit for inside measurement.

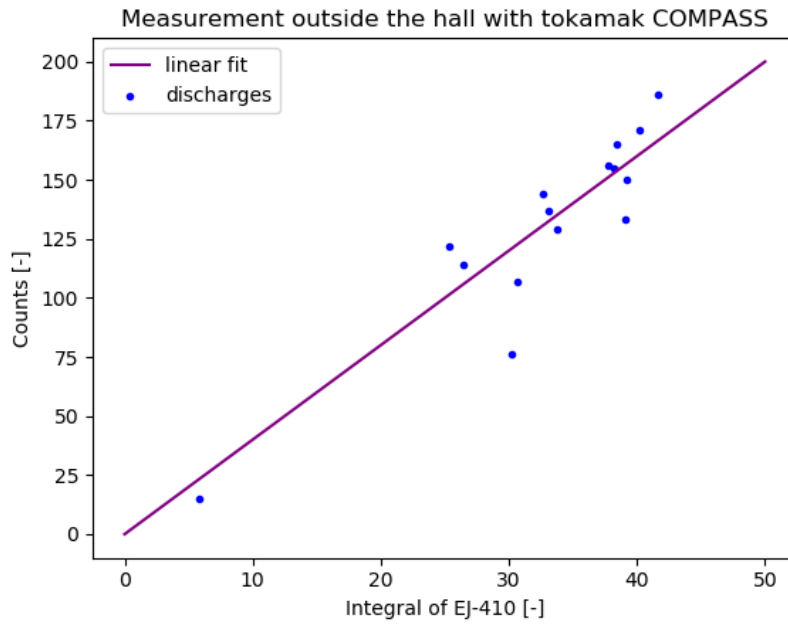


Figure 2.4: Linear fit for outside measurement.

- K_n should be probably higher due to moderating neutrons by wall.
3. The cross section of the human body (worker) is about 1 m^2 and the weight is about 80 kg.
 4. All passed neutrons through the shielding wall have energy 25 keV. The

reason is as follows. Attenuation coefficient K_n says to us, that only one neutron passed through the wall on each 84 neutrons, which are absorbed (or reflected back). The neutron absorption in the wall in particular takes place in such a way, that fast neutrons are slowly moderated during elastic collisions with material nuclei. After slowing down on ideally thermal energies, neutrons are absorbed in the material (because of high cross section of absorption for slow/thermal neutrons). It can be thus assumed, that the one neutron passed through the wall will be strongly moderated too in each case. For strong upper estimate let's say the passed neutrons are minimally 100 times slowed, this is energy of 25 keV. The smaller the energy will be, the smaller will be the absorbed dose. So this is ideal for strong upper estimate of the absorbed dose. The cross section for nuclear reaction of neutron with 25 keV with ^6Li is about 1 barn, based on figure 1.1.

5. Radiation weighting factor $W_R = 10$. It corresponds approximately to neutron with energy 25 keV, [6].

6. All neutron radiation, which entered into the human body, is completely absorbed, none goes through.

■ 2.3.1 Equivalent dose of the COMPASS tokamak

For the estimation of equivalent dose, the efficiency of detection of 25 keV neutron by NuDET detector was first calculated, see the chapter 1.2. After this it is simple to calculate number of neutron counts for the whole year. Finally equivalent dose for tokamak COMPASS H_C , eq. 1.3, was determined as

$$H_C = 596,25 \text{ } \mu\text{Sv/year.} \quad (2.7)$$

Allowed equivalent dose for worker with ionizing radiation is 50 mSv/year (for general public 2 mSv/year). H_C is **than 84x lower than set limit**. Let's take note, that it is strong upper estimate. The true equivalent dose should be much lower.

■ 2.3.2 Equivalent dose of the COMPASS-U tokamak

For the estimation of equivalent dose for COMPASS-U the same assumptions like for COMPASS were used, but with two changes. Every discharge will generate $\sim 3 \cdot 10^9$ neutrons registered in NuDET detector inside. It means up to 10^5 higher the amount of neutrons from COMPASS-U than from COMPASS (by 10^4 higher neutron fluxes and the duration of NBI heating phase will be 10x longer).

The second change is in the neutron attenuation coefficient. The shielding

wall of COMPASS-U will be composed of old 60 cm thick concrete wall from COMPASS and from additional 90 cm thick layer of new concrete with boron. So the COMPASS-U will be shielded by 150 cm thick concrete wall. This wall should reduce neutron fluxes by around six orders of magnitude ($K_n = 10^6$), see the figure 2.5. Note, that the reduction of absorbed dose by 60 cm thick concrete is about 2 orders of magnitude in this figure, which well corresponds with our measurement of neutron attenuation coefficient, so the use of the results from this figure from [2] is reasonable.

The equivalent dose for COMPASS-U is than

$$H_{C-U} = 5,01 \text{ mSv/year.} \quad (2.8)$$

This equivalent dose is 10x lower than set limit. Again, it is very strong upper estimate. The true equivalent dose should be much lower. Moreover, the structures of the COMPASS-U will have radically higher radiation shielding ability by itself than structures of COMPASS and the additional boron concrete will probably have better shielding properties than ordinary concrete. These facts are not taken into account in this calculation and thus should rapidly decrease the true equivalent dose, too.

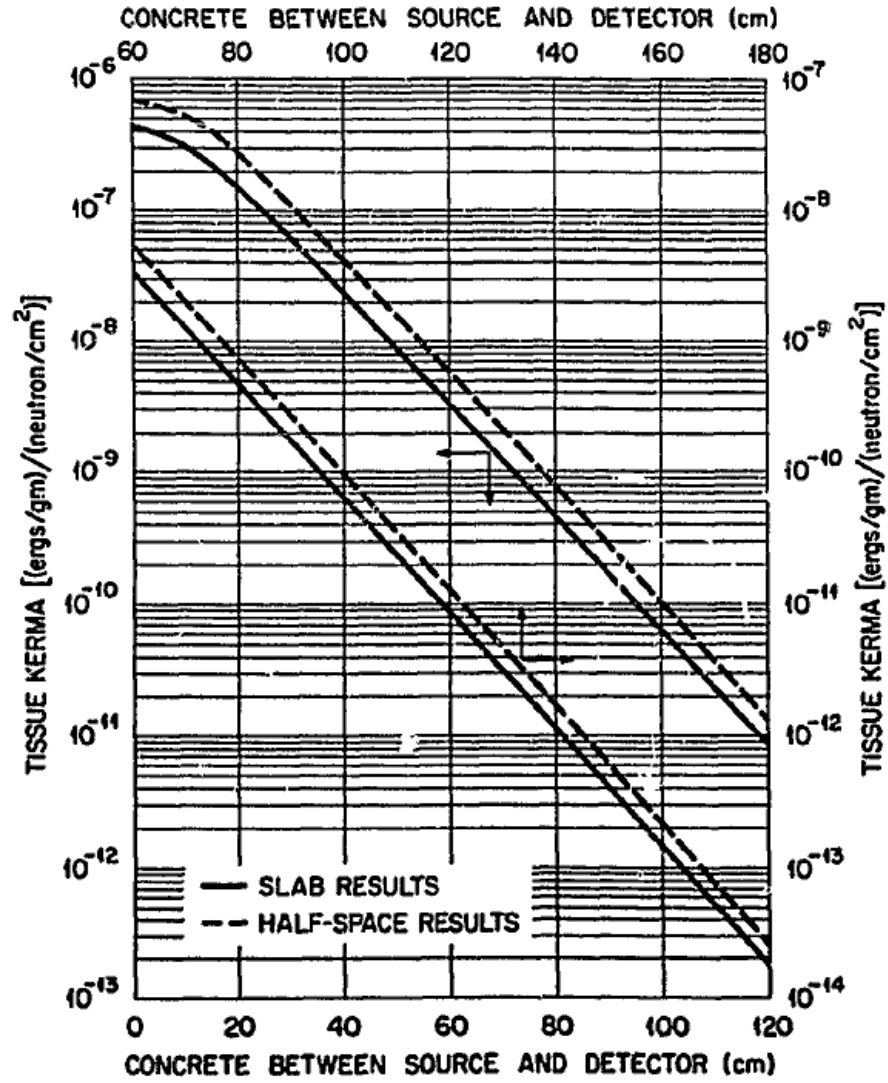


Figure 2.5: Reduction of absorbed dose by ordinary concrete shielding from 3 MeV incident neutrons, [2].

Chapter 3

Measurement of neutrons on the HXR background

Measurements of neutron fluxes on the tokamaks (and other fusion devices) are a very useful tool and especially with growing size and fusion power of the newly built tokamaks, the neutron diagnostics is becoming more and more important. Most of neutron detectors used for measurement of high neutron fluxes like scintillators are also sensitive to HXR/ γ radiation. It can be a big disadvantage, but not in the case, that we are able to separate them from neutrons (neutron/HXR discrimination).

3.1 Experimental setup

To explore neutron/HXR discrimination capabilities of NuDET scintillator detector we have realised measurement during runaway electron campaign CC22.01 in January/February 2020. Runaway electrons are the strong source of HXR radiation. It was our goal to measure individual HXR peaks, although NuDET cannot provide any energy resolution. NuDET detector was thus placed behind the main wall around tokamak COMPASS. Without shielding wall NuDET wouldn't be able to measure individual HXR photons due to too large HXR flux (piled-up signal). NuDET was connected to the OWON oscilloscope XDS3202A with necessary low impedance ($Z = 50 \text{ Ohm}$) and fast sampling rate from 50 to 250 MHz.

■ 3.2 Measurement of HXR counts

We have measured with a lot of different oscilloscope input parameters for better understanding of the measured signal and for finding ideal oscilloscope setup for these types of measurements. So the data are not self-consistent for some big statistical analysis, but we still have obtained important informations about the time dimension and the shape of HXR peaks (see below) at different oscilloscope parameters like vertical resolution, sampling rate and bandwidth.

The shielding wall really shielded HXR to such an extent, that we could recognise individual HXR peaks, figures 3.1 and 3.2. Numbers of counts vary in quite wide range from a few thousands up to more than 1 million HXR counts registered in NuDET detector per discharge. Complete list of used discharges with specific numbers of counts is shown in the tables 3.2 and 3.3. Calculating the estimate of absolute numbers of HXR generated by tokamak during discharge is impossible now, because there is still a lot of unknown quantities like HXR wall absorption, HXR spectrum. Unfortunately, neither NuDET sensitivity to HXR is known, respectively it is „low“. It's quite obvious, because NuDET scintillation crystal has very small volume. Typical scintillation crystals for measuring HXR/ γ like NaI(Tl) are manufactured in larger volumes.

■ 3.2.1 Equivalent dose from RE discharges

Comparing these numbers of HXR counts with neutron counts in the chapter 2 leads to the conclusion, that equivalent dose during RE discharge is approximately 3 orders of magnitude higher than the one from neutron discharge (10^4 higher counts - more than a million HXR vs several hundred neutrons, but radiation weighting factor W_R is 10 times lower for HXR than for neutrons). Moreover, NuDET sensitivity to HXR radiation is in general „low“. This fact can further increase the difference between equivalent doses between REs and neutrons. Generally speaking, the individual RE discharges can thus significantly increase equivalent dose of radiation from the tokamak.

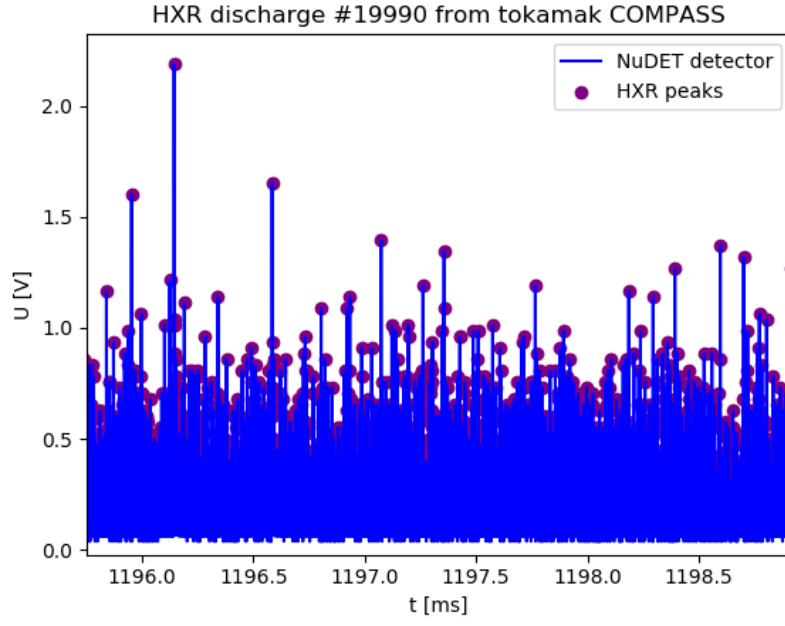


Figure 3.1: Example of the cluster of HXR peaks.

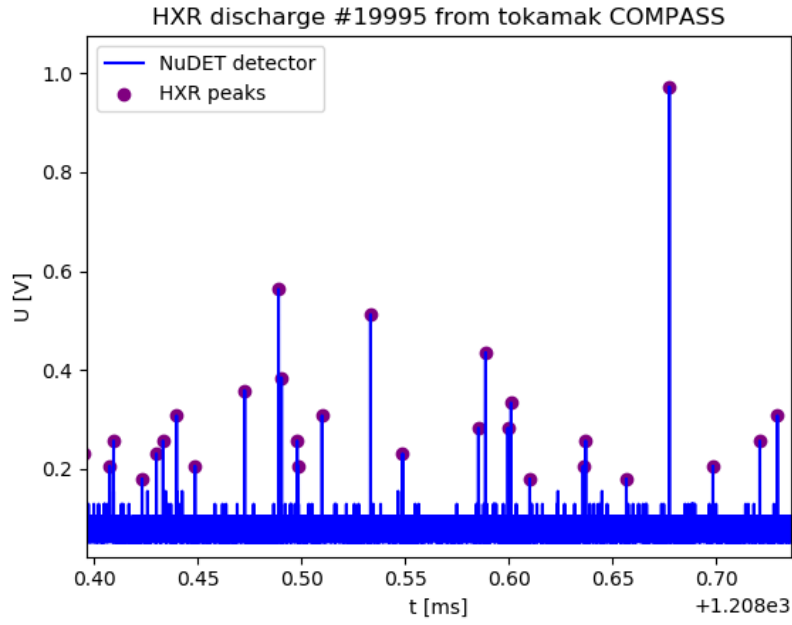


Figure 3.2: Example of HXR peaks (enlarged area).

3.3 Neutrons discovery

During a detailed study of the HXR signal from NuDET detector we have noticed a few very different peaks. Detailed view on the figures 3.3 and 3.4 shows a substantial difference between representatives of both groups. Notice, that time axis has different units (ns vs μ s). Many HXR peaks appear here as a quite big noise of this signal and thus can be interpreted as some random pile-up effect. Due to this fact the analysis of this signal was done.

Representative peaks of both groups were fitted, as we can see on the figures 3.3 and 3.4. Results of fits were compared with the article [12], where author used similar type of scintillation detector (ZnS(Ag) + LiF). HXR peak was fitted with 1 exponential function (fast component only). Unknown peak was fitted with the sum of 3 exponential functions (fast, slow, ultraslow component). Decay times of individual components are shown in the table 3.1. Ratios of individual decay times are almost the same, ultraslow component is a bit slower, it's due to a lot of HXRs in the tail of the neutron peak. Absolute differences are due to different electronics used (PMT, oscilloscope). In conclusion it can be said, that these different peaks are certainly the neutrons and not some piled-up signal.

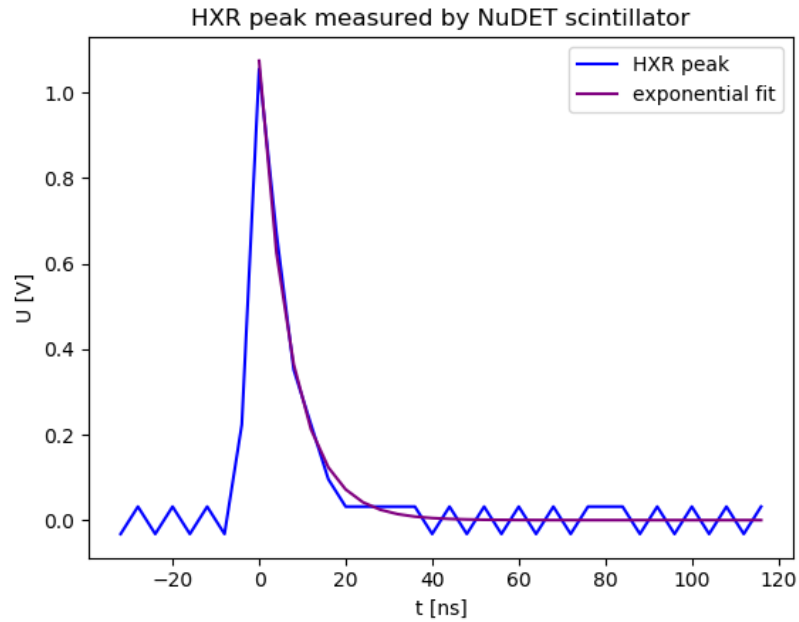


Figure 3.3: Example of the HXR peak.

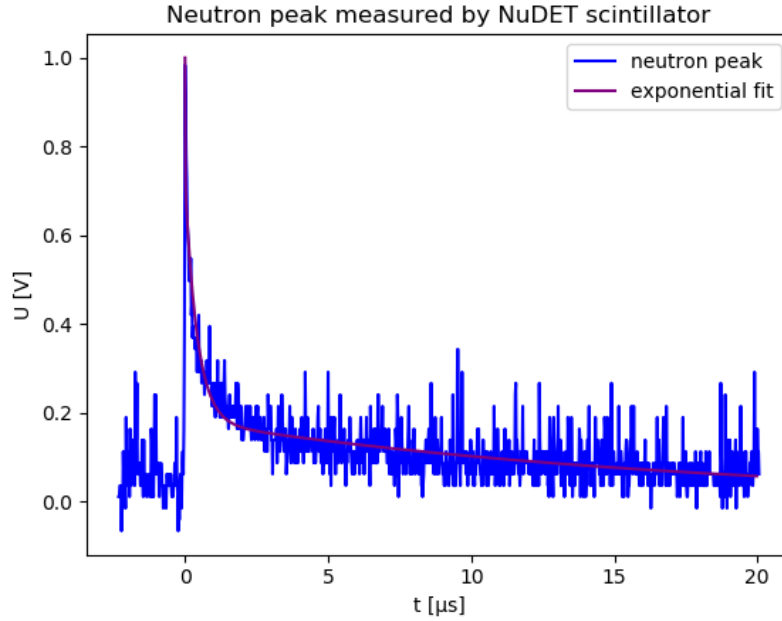


Figure 3.4: Example of the neutron peak.

	OUR FIT [μ s]	ARTICLE FIT [μ s]
HXR τ_1 (fast)	0,008	0,003
neutron τ_1 (fast)	0,008	0,003
neutron τ_2 (slow)	0,424	0,160
neutron τ_3 (ultraslow)	17,367	4,100

Table 3.1: Time decays of HXR and neutron peak.

3.4 Source of neutrons

3.4.1 Neutron/HXR discrimination

For the determination of the neutron source, it was necessary to separate neutron peaks from HXRs. By using Fourier transform of the exponential function (eq. 1.6 and 1.7) the spectral decompositions of neutron/HXR peaks were calculated, figures 3.5 a 3.6. Due to very different decay times their FWHM are greatly different. This fact allowed us to discriminate neutrons from HXR peaks by using 100 kHz lowpass bandwidth filter. As we can see in the figures 3.7 and 3.8, HXR peak is completely filtered out and only ultraslow component of the neutron peak has passed the filter.

This discrimination method is simple to use and thus it's a good choice

in the situations like this with very different decay times of neutron/HXR peaks. In other types of scintillation detectors like plastic, neutron and HXR peaks can be much more similar, there it would be necessary to use some sophisticated discrimination techniques like Pulse Gradient Analysis (PGA), Charge Comparison Method (CCM), see e.g. [5].

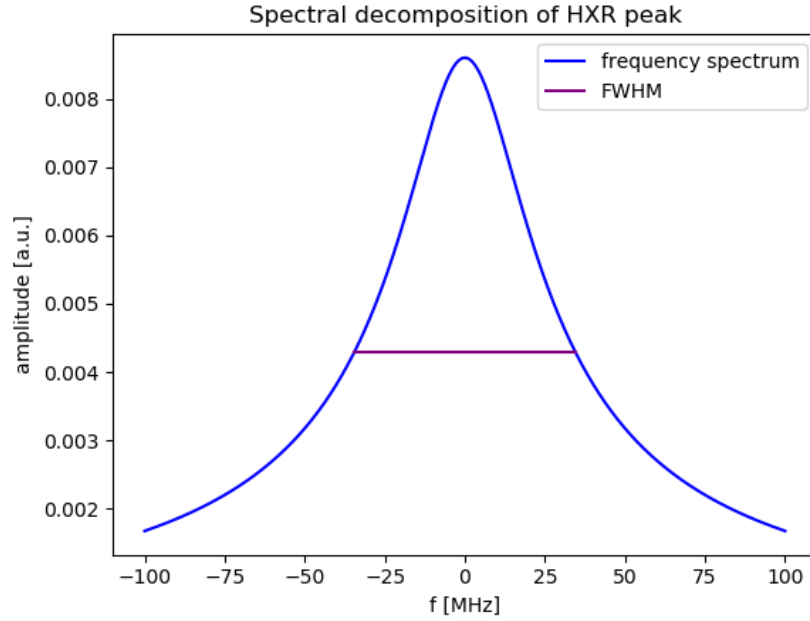


Figure 3.5: Spectral decomposition of HXR peak.

3.4.2 Neutron counts

In the tables 3.2 and 3.3, there is a list of discharges, where we have measured high HXR fluxes. Discharges were separated into two groups according to the number of neutron peaks detected. We have especially compared discharges #19985 vs #19997, in both discharges NuDET detected approximately $5 \cdot 10^5$ HXR counts, but neutron flux was quite different (71 vs 2 neutrons). **We have discovered, that high neutron fluxes exist due to deuterium gas puff during the runaway electron beam phase.** Notice, that these neutron fluxes are similarly high like from a D-D fusion discharges in the COMPASS tokamak, see the figure 2.4.

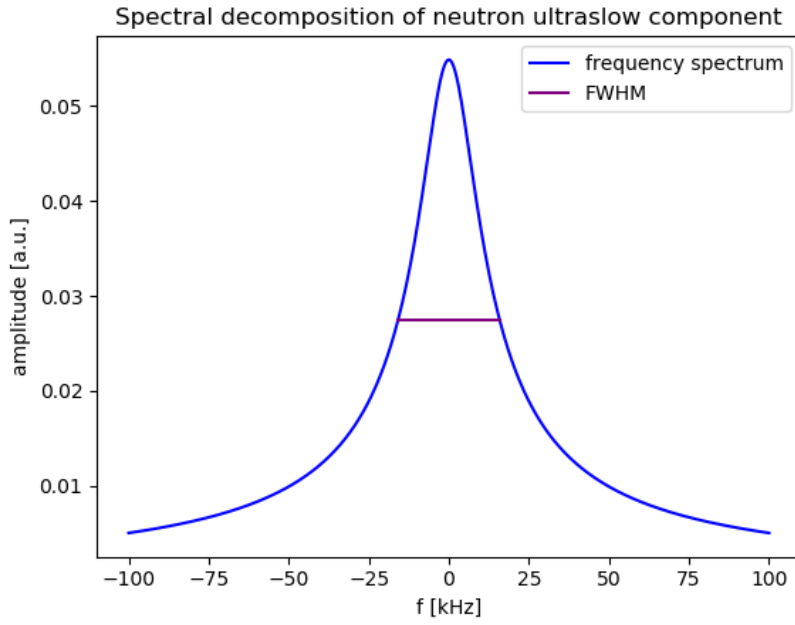


Figure 3.6: Spectral decomposition of neutron ultraslow component.

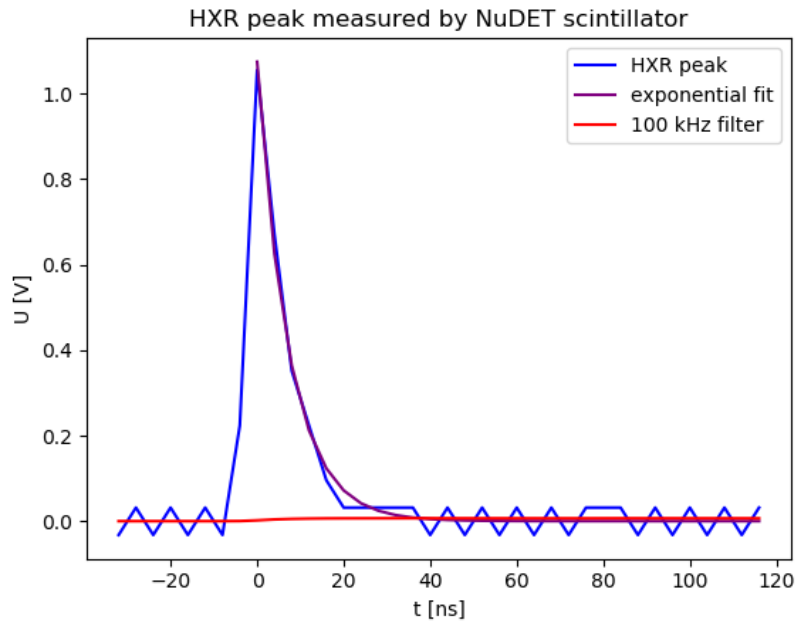


Figure 3.7: Application of 100 kHz lowpass bandwidth filter on HXR peak.

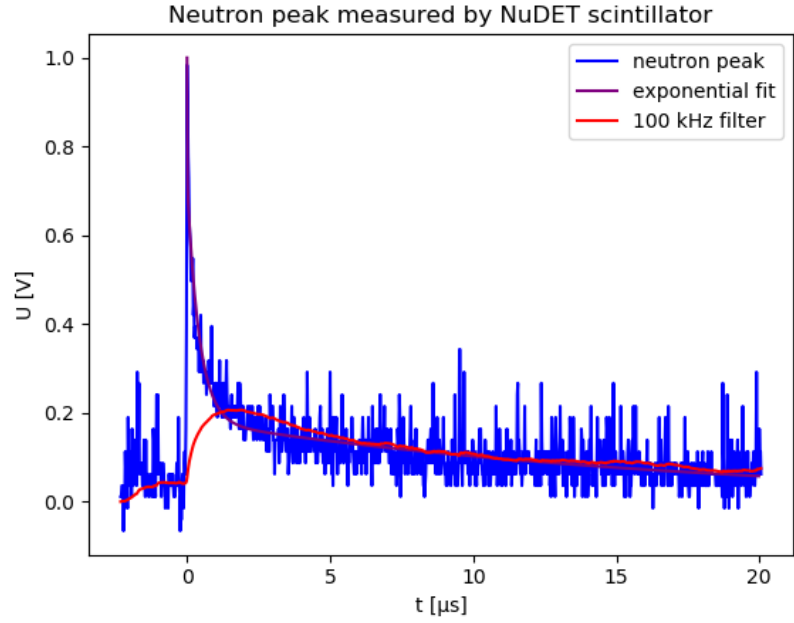


Figure 3.8: Application of 100 kHz lowpass bandwidth filter on neutron peak.

DISCHARGE	HXRS	NEUTRONS	D PUFF
19984	57776	35	YES
19985	504075	71	YES
19990	1095793	146	YES
19991	852639	136	YES
20005	1007070	95	YES

Table 3.2: The list of discharges with high neutron fluxes.

DISCHARGE	HXRS	NEUTRONS	D PUFF
19995	205998	2	NO
19996	495515	4	NO
19997	526819	2	NO
19998	200114	5	NO
20007	70950	1	NO
20010	157872	0	NO
20021	137466	0	NO
20036	61236	1	NO
20040	66851	1	NO
20042	59570	0	NO
20077	73089	0	NO

Table 3.3: The list of discharges without or with very low neutron fluxes.

3.4.3 Deuterium gas puff

Neutrons presence in the signal after deuterium gas puff in the tokamak means, that we dominantly detect nuclear reaction



This phenomenon is called photodisintegration, see [3]. It's an endothermic reaction with the threshold $E_\gamma \simeq 2,2$ MeV with maximum cross section about $\sigma \simeq 0,0025$ barn, figure 3.9. **Measurement of these photoneutrons can thus be used as a proof of the presence of runaway electrons with energies higher than 2,2 MeV.**

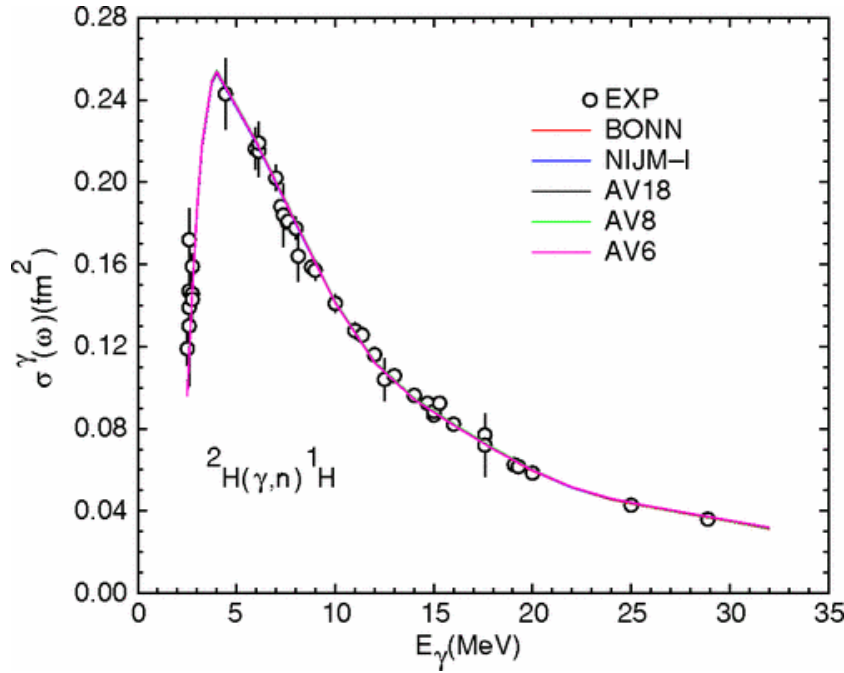


Figure 3.9: Cross section of the $D(\gamma, n){}^1\text{H}$ reaction, [3].

The measurement of photoneutrons from various photodisintegration reactions was also realised on the JET tokamak, see [13]. For more detailed informations about photoneutron sources, see the papers [14, 15].

■ Estimation of number of HXR photons generated by runaway electrons

Moreover, the fact that we know absolute numbers of neutrons and the main source of them give us the possibility to calculate rough estimate, how

many HXR photons with energies more than 2,2 MeV are generated during the decay of the RE beam.

The main assumptions for this estimation are as follows:

1. Tokamak is like spherical isotropic source of photoneutrons.
2. Average track of HXR photon through the plasma is approx. 20 cm, than HXR photon leaves the plasma.
3. We consider the maximal cross section of the reaction $D(\gamma, n)^1H$, $\sigma = 0,0025$ barn.
4. All photoneutrons are thermalized ($E = 0,025$ eV) behind the wall. This leads to assume the maximal cross section of the reaction ${}^6Li(n, \alpha)T$.
5. We consider the case with the highest measured neutron flux and HXR (discharge #19990).

The assumptions 1. and 2. are used to simplify the calculation. In fact, we don't have necessary informations for more accurate model. The assumptions 3. and 4. suppose the maximum effectivity during whole process and thus lead to the bottom rough estimate of the number of HXR. The fifth assumption means, that we focus on disruptions with the most runaway electrons.

By using the assumptions 1. and 4. was calculated

$$N_n = 2,4 \cdot 10^{10}, \quad (3.2)$$

where N_n is the total number of neutrons generated by HXR-D photodisintegration reactions. Then, the number of HXR in the plasma was simply calculated from the definition of the cross section, eq. 1.1. Here, the number of reactions was N_n , the cross section was taken from the assumption 3. We have considered the approximation, that the HXR flux hits the target, which is a cube with 20 cm length (the second assumption) filled with deuterium gas (deuterium nuclei density $\sim 10^{20}$). It is due to the definition of the cross section.

The result is, that the runaway electrons in the strong disruptions can generate minimally $4 \cdot 10^{21}$ HXR photons with energies more than 2,2 MeV. Without any further details it can be said, that this number is generally by a few orders of magnitude higher than is expected from the existing knowledge about runaway electrons on the COMPASS tokamak. Note, that when imagining a target more like a toroid, the result is almost the same. One of the possible facts, that is not taken into account, is, that HXR should probably pass through the plasma repeatedly due to Compton scattering. This fact would lead to decrease this estimate, but probably not enough. There may be a problem with the assumption of isotropy, too. Further investigation of this incompatibility is needed.



Conclusion

Due to the fact, that COMPASS tokamak will close soon, our interest was focused on the use of the last campaigns to collect data of individual peaks of neutrons and HXR photons by NuDET scintillation detector.

COMPASS campaign CC21.06 gave us the opportunity to measure absolute numbers of neutron fluxes behind the main shielding wall around tokamak during standard NBI discharges. Using older measurement of neutron fluxes inside the hall of the tokamak, it was calculated that the neutron wall attenuation coefficient is $K_n = 84$. This is the minimal shielding ability of the wall. This means, that the wall reduces neutron fluxes by about two orders of magnitude. Then, the rough upper estimate of equivalent dose outside the experimental hall of the COMPASS tokamak was determined as $H_C = 596,25 \mu\text{Sv}$ per year. It is 84x lower than the legal limit of 50 mSv per year. Finally, the estimate of equivalent dose of the COMPASS-U tokamak was calculated. Despite of up to 10^5 times higher neutron counts the equivalent dose of COMPASS-U was determined as only $H_{C-U} = 5,01 \text{ mSv}$ per year. It is due to a far better wall shielding of COMPASS-U than the current shielding available on COMPASS. This result is 10x lower than the legal limit. Note, that this is a strong upper estimate of equivalent dose. The real equivalent dose of COMPASS-U will be probably much lower.

During RE campaign CC22.01 the main shielding wall around COMPASS tokamak reduced HXR flux from runaway electrons enough, that individual HXR peaks were recognizable. NuDET detector measured up to more than 10^6 HXR peaks per discharge in some cases. Given these numbers and comparing them with neutron fluxes in standard NBI discharges, it's obvious, that a few RE discharges can distinctly increase equivalent dose per year produced by the COMPASS tokamak.

During a detailed analysis of the shapes of measured HXR peaks, a few significantly different peaks were found. Then, it was clearly verified, that we

have measured unexpected neutron fluxes in similar magnitudes like in NBI discharges. It is understood, that these are photoneutrons originating from γ -deuterium photodisintegration nuclear reaction, which is the proof of the presence of runaway electrons with energies higher than 2.2 MeV by itself.

Using a simple model, it was calculated, that the runaway electrons should generate minimally $4 \cdot 10^{21}$ HXR photons with energies more than 2,2 MeV in order to explain the observed photoneutron fluxes. This estimate is generally by a few orders of magnitude higher, than is expected. One of the next steps should be to find out the reason of this incompatibility with existing knowledge about runaway electrons, whether it is some essential mistake in our calculation or this result points to something overlooked in the RE physics. For example, HXRs should probably pass through the plasma repeatedly due to Compton scattering, which would lead to decrease this estimate. Alternatively, the assumption of isotropy is not entirely real, and thus the detector was accidentally placed in some preferred direction.

Similar measurements could be made on the GOLEM tokamak at FJFI CTU in Prague. The existence of the runaway electrons with energies higher than 2,2 MeV on the COMPASS tokamak is quite obvious even without this measurement, but on the GOLEM tokamak it is very questionable and thus the attempt of measurements of photoneutrons on the GOLEM tokamak could be very interesting.

In this work, it was proven, that NuDET detector has possibility to measure photoneutrons, respectively the discrimination of neutrons from HXR/ γ radiation is feasible. It could be than possible to measure more interesting photodisintegration nuclear reactions like $^{208}\text{Pb}(\gamma, n)^{207}\text{Pb}$, which has higher energy threshold $E_\gamma \doteq 7,4$ MeV, [16].



Appendix

Due to the scope of the assignment, author's interest was naturally focused on the time-limited goals connected with the approaching closure of the COMPASS tokamak. So thus the realisation of a few last neutron/HXR measurements was our priority. Then, the data analysis of the measured signals was naturally the next step, connected with the development of neutron/HXR discrimination abilities, which was one of the goals of the research task, too.

The supervisor, Ondřej Ficker, took care of the theoretical issues like the influence of neutron source toroidal geometry and the neutron energy distribution function on the measured neutron fluxes and the group of researchers from the Institute of Nuclear Research of the Polish Academy of Sciences conducted the first simulation of the COMPASS-U neutron transport using the MCNP6 code. In this section, some aspects of these topics important for the complete understanding of the working principles of the neutron diagnostics, are presented.

■ Analytical verification of influence of toroidal neutron source geometry on the detected neutron fluxes

In a few previously presented calculations, the assumption of spherical isotropic source of neutrons was used to simplify the calculations. Actually, this geometry assumption is too simplified - the realistic shape of the source is not a point but a toroid and there are also scattered neutrons. For the illustration of the work of Ondřej Ficker, the figure 3.10 shows radial profile of neutron flux in height of 0,6 m over the equatorial plane of the COMPASS

tokamak. The difference between the toroidal source geometry and the point source approximation is obvious.

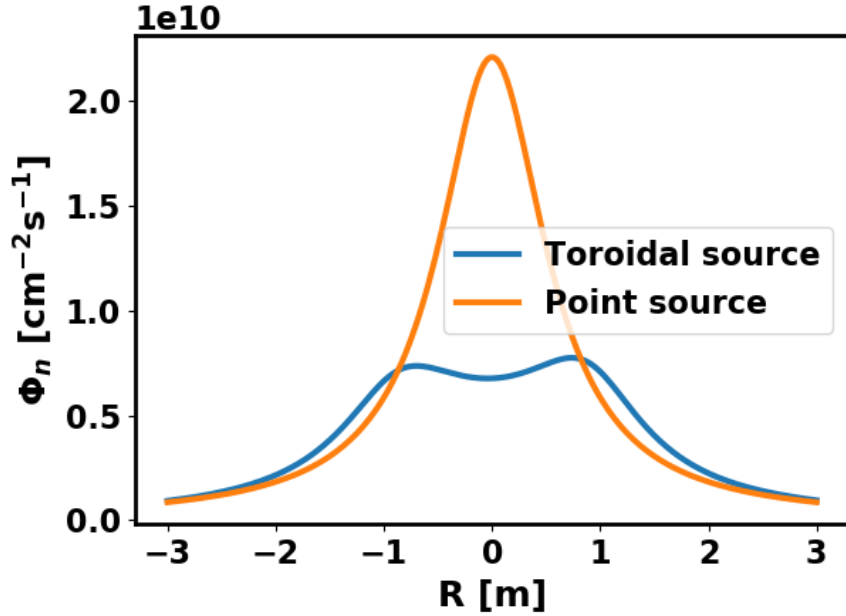


Figure 3.10: Radial neutron profile of a toroidal sources in a size of the COM-PASS tokamak plasma, author: Ondřej Ficker.

■ Influence of energy distribution function of neutrons and detector attributes on the detected neutron fluxes

Not only neutron source geometry, but also neutron energy distribution function and the detector attributes have the influence on the measured neutron fluxes. In the calculations presented in chapters 2 and 3, the Dirac delta function is factually considered as the neutron energy distribution function, which is useful in the situations of calculating limit value of some quantity like equivalent dose, number of HXRs. For the calculation of the real values, not only limit values, the knowledge of the parameters of the real neutron energy distribution function is necessary.

Under the words „detector attributes“, the wide range of the values of the cross section of selected nuclear or another reaction (like ${}^6\text{Li}(n, \alpha)\text{T}$ in NuDET) is mainly understood. Together, we can get more precise numbers of neutron counts. For the illustration, the figure 3.11 shows the dependency of neutron fluxes on the Gaussian neutron energy distribution function with the given mean value of the neutrons energy.

■ Neutron transport in the COMPASS-U tokamak

Group of researchers from the Institute of Nuclear Research of the Polish Academy of Sciences has been working lately on the modelling of the neutron transport in the COMPASS-U tokamak experimental hall. In the figure 3.12, the small illustration of their work is presented. The figure shows a vertical section of the COMPASS-U with calculated neutron fluxes per year. There is clearly shown, that COMPASS-U structures will significantly shield neutron radiation by about two orders of magnitude. Additional shielding provides also a built-in floor, on which various auxiliary systems will be standing.

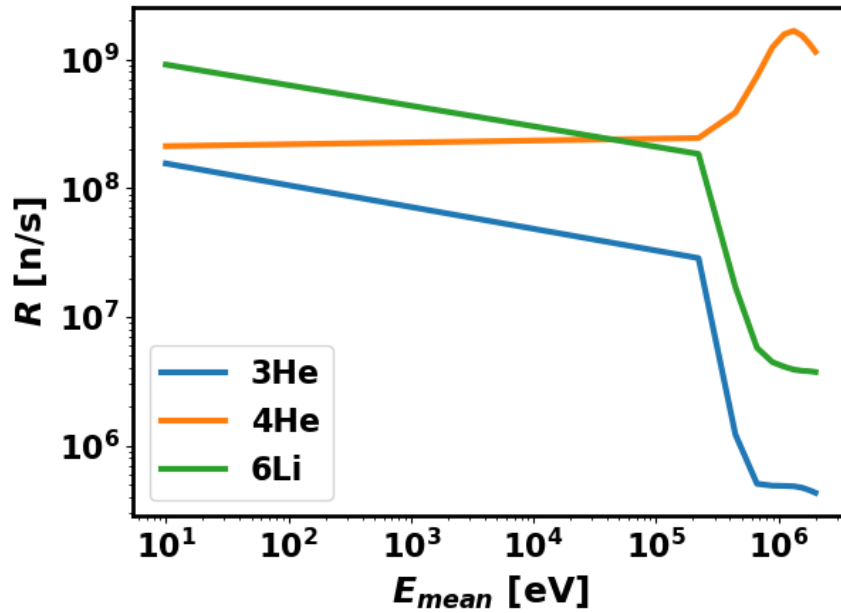


Figure 3.11: Dependency of the neutron count rate on the mean energy of neutrons for the three different reactions ($^6\text{Li}(n, \alpha)\text{T}$; $^3\text{He}(n, p)^3\text{H}$; $n - ^4\text{He}$ recoil), author: Ondřej Ficker.

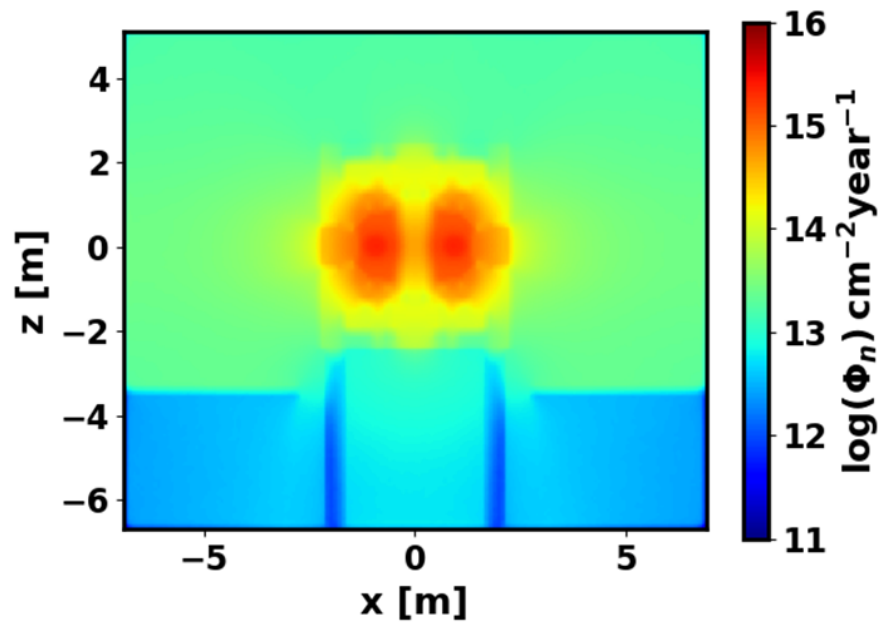


Figure 3.12: Order of magnitude of neutron fluxes per cm^2 per year of the COMPASS-U tokamak, author: group of researchers from the Institute of Nuclear Research of the Polish Academy of Sciences.



Bibliography

- [1] M. Pickrell, A. Lavietes, V. Gavron, D. Henzlova, M. Joyce, R. Kouzes, and H. Menlove, “The iaea workshop on requirements and potential technologies for replacement of 3He detectors in iaea safeguards applications,” *JNMM, Journal of the Institute of Nuclear Materials Management*, vol. 41, pp. 14–29, 03 2013.
- [2] F. A. R. Schmidt, “THE ATTENUATION PROPERTIES OF CONCRETE FOR SHIELDING OF NEUTRONS OF ENERGY LESS THAN 15 MeV,” tech. rep., OAK RIDGE NATIONAL LABORATORY, 1970.
- [3] R. Schiavilla, “Induced polarization in the ${}^2\text{H}(\gamma, \vec{n}){}^1\text{H}$ reaction at low energy,” *Phys. Rev. C*, vol. 72, p. 034001, Sep 2005.
- [4] J. Mlynář, “Fúzní jaderné reakce,” 2018. Přednáška a powerpointová prezentace k předmětu Úvod do termojaderné fúze na FJFI, ČVUT.
- [5] L. Lobko, “Měření neutronů na tokamaku COMPASS,” 2019.
- [6] W. Muhammad, A. Hussain, and M. Maqbool, *Basic Concepts in Radiation Dosimetry*, pp. 9–41. 11 2017.
- [7] H. Shatkay, “The fourier transform – a primer,” 10 1996.
- [8] O. Ficker, “Generation, losses and detection of runaway electrons in tokamaks,” Master’s thesis, FJFI CVUT, 2015.
- [9] C. Liu, *Runaway electrons in tokamaks*. PhD thesis, Princeton university, 2017.
- [10] O. Ficker, E. Macusova, J. Mlynář, D. Bren, A. Casolari, J. Cerovsky, M. Farník, O. Grover, J. Havlicek, A. Havranek, M. Hron, M. Imrisek, M. Jerab, J. Krbec, P. Kulhanek, V. Linhart, M. Marcisovsky,

- T. Markovic, D. Naydenkova, and C. Reux, “Runaway electron beam stability and decay in compass,” *Nuclear Fusion*, vol. 59, 05 2019.
- [11] O. Ficker, “Neutron measurements at COMPASS,” 2019. Powerpointová prezentace.
- [12] F. Pino, L. Stevanato, D. Cester, G. Nebbia, L. Sajó-Bohus, and G. Viesti, “Study of the thermal neutron detector ZnS(Ag)/LiF response using digital pulse processing,” *Journal of Instrumentation*, vol. 10, pp. T08005–T08005, 08 2015.
- [13] O. Jarvis, G. Sadler, and J. Thompson, “Photoneutron production accompanying plasma disruptions in JET,” *Nuclear Fusion*, vol. 28, p. 1981, 01 2011.
- [14] A. Wattenberg, “Photo-neutron sources and the energy of the photo-neutrons,” *Phys. Rev.*, vol. 71, pp. 497–507, Apr 1947.
- [15] D. Salehi, M. Jozani, and D. Sardari, “Characteristics of a heavy water photoneutron source in boron neutron capture therapy,” *Chinese Physics C*, vol. 37, 07 2013.
- [16] B. Ishkhanov, V. Orlin, and S. Troschiev, “Photodisintegration of Pb isotopes,” *Moscow University Physics Bulletin*, vol. 66, pp. 135–141, 04 2011.